JOURNAL OF OPTOELECTRONİCS AND ADVANCED MATERİALS Vol. 9, No. 7, July 2007, p. 2186 - 2191

Influence of the thickness on physical properties of chemical bath deposited hexagonal ZnS thin films

F. GÖDE, C. GÜMÜŞ[a*], M. ZOR
Physics Department, University of Anadolu 26470 Eskişehir, Turkey
[a]Physics Department, University of Cukurova 01330 Adana, Turkey

Hexagonal ZnS thin films of thicknesses ranging between 454 to 750 nm are deposited on a glass substrate by chemical bath deposition at 80 ºC. The ZnS thin films are characterized by X-ray diffraction (XRD) and optical absorption spectroscopy. The films are shown to be crystallized in the hexagonal phase and present a preferential orientation along the *c*-axis by XRD measurements . Only one peak, corresponding to the (008) phase (2θ=29.5º), appears on the diffractograms. The ZnS films show a high transmission. The optical constants such as refractive index *n*, extinction coefficient *k*, real ε_1 and imaginary ε_2 part of dielectric constant are calculated in the visible region. A reduction in refractive index (*n*) and the extinction coefficient (*k*) is observed as film thickness decreases. The electrical conductivity decreased from 1.62×10^{-9} to 1.32×10^{-10} $(\Omega.cm)^{-1}$ when the films are annealed at 400 ºC for 1 hour. The temperature-dependent current was measured in the range 27-400 ºC and the activation energy values were obtained using the temperature-dependent current measurements.

(Received June 4, 2007; accepted June 27, 2007)

Keywords: Chemical bath deposition, ZnS, Refractive index, Electrical conductivity, Activation energy

1. Introduction

Generally in thin film solar cells based on $CuInS_2$ (CIS), $CuInSe_2$ (CISe) and $Cu(In,Ga)(SSe)_2$ (CIGSSe), a CdS buffer layer deposited by chemical bath deposition (CBD) is required on the device to obtain high conversion efficiencies. There are, however, toxic hazards with respect to the production and use of the CdS layer. This issue has stimulated much research in developing Cd-free buffer layers. This has primarily been investigated using ZnS as a buffer layer in $CuInSe_2$ based devices [1]. ZnS is also an important semiconducting material, used in wave-guides, blue light emitting devices and as a base material for the phosphors.

The refractive index (*n*) of a material is the key parameter for device design [2], because it is closely related to the electronic polarizability of ions and the local field inside the material. Evaluating the refractive index of optical materials is of considerable importance for applications in integrated optical devices such as switches, filters, modulators, and heterostructure lasers [3] etc. Consequently, there have been many theoretical and experimental works in literature related to the refractive index of the cubic ZnS. In the theoretical work, Rabah et al [4] found the refractive index of cubic ZnS to be 2.25 using the self-consistent scalar-relativistic full potential linear-augmented plane wave (FP-LAPW) method. Using Successive Ionic Layer Adsorption and Reaction (SILAR) [5] method on a glass substrate at room temperature, the refractive index of cubic ZnS film was found between 1.95 and 2.23. Ibanga et al [6] found the refractive index of cubic ZnS films deposited on glass substrates at 40 ºC by CBD method to be 1.96. Using glancing angle deposition (GLAD) technique, Wang et al [7] obtained the maximal and minimal refractive index values of the cubic ZnS films as 2.15 and 2.11 respectively. The refractive index values of cubic ZnS films on a (100) GaAs substrate at room temperature using SILAR increased from 1.63 to 2.17 [8] as the film thickness increased from 35 nm to 136 nm.

The focus of this work is on the preparation of ZnS thin films of different thicknesses deposited onto a glass substrate by CBD at 80 ºC. Results for the refractive index (*n*), extinction coefficient (*k*), and the real (ε_1) and imaginary (ε_2) parts of the dielectric constant are also included in this report. It should be noted that although there are many works on the refractive index of cubic ZnS, there are limited articles on the refractive index of the hexagonal ZnS. The electrical conductivity values have been evaluated before annealing and after annealing at 400 ºC for 1 hour. Activation energies of the hexagonal ZnS thin films were calculated from the temperature-dependent current measurments.

2. Experimental details

ZnS thin films were produced by CBD on glass substrates. The substrates used for the deposition of ZnS thin films were glass slides with the dimensions $76 \times 26 \times 1 mm^3$. Before deposition, the substrates where etched with diluted hydrochloric acid (5 %), cleaned in deionized water and then cleaned with propanol, methanol and again washed with deionized water before it was finally dried by air. To obtain ZnS thin films, the solution was prepared by mixing 2.5 ml of 1 M Zn $(CH_3COO)_2$, 0.5 ml of 3.75 M triethanolamine (TEA), 2.5 ml ammonia/ammonium chloride (NH_3/NH_4Cl, pH=10.55) buffer solution, 0.8 ml of 0.66 M tri-sodium citrate ($C_6H_5Na_3O_7$), 2.5 ml of 1 M thiourea, deionized water was added to make the total volume of the solution 20.8 ml. The mixture was poured into a beaker and heated to 80 °C.

The process consisted of an aqueous bath heated by a hot plate who's temperature controller had an acuracy of ±2°C. When the deposition temperature was reached, four precleaned glass slides were introduced into the solution and left for deposition times of 3.0, 3.5, 4.0 and 4.5 hours to get achieve different thickness films. In order to get thicker films, the solution which was in the same condition before the substrates were dipped was added to the reaction bath because of the evaporation of water in aqueous solution. After the glass substrates were removed, they were washed with tap water, rinsed in deionized water to remove soluble impurities and then dried in the air. The ZnS thin films deposited on the glass slides were green and pink in colour. In all the film preparation, the glass substrates were put vertically on the side of the beaker. To enable the optical absorption, the films grown on the back side were removed by cotton swabs dipped in concentrated HCl.

Gold (Au) contacts were made by vacuum evaporation to allow measurement of the *I-V* characteristics of the films. In order to measure the activation energies, the film was put into the oven and connected to a power supply with a heat-resistant silicon cable. Silver paste was used to make a connection from silicon cable to the film. The film was then heated to 400 ºC. During heating, the voltage was held constant at 20 V and the corresponding output current was measured by digital multimeters. The temperature-dependent current of the ZnS film was recorded for the range 27-400 ºC. These measurements were performed in the dark to eliminate photoconduction.

The X-ray diffraction (XRD) patterns were recorded to characterize the phase and structure of the nanoparticles using Rigaku Rint 2000 X-ray diffractometer with a rotating anode and a Cu-Kα_1 radiation source (λ=0.15406 nm) at 40 kV and 30 mA. Optical transmission data was obtained with a Shimadzu UV-2101PC scanning spectrophotometer. The current-voltage (*IV*) measurements were performed using HP4140B pA meter/DC voltage source, HP34401 Model Digital multimeter and Vee One Lab 6.1 computer program. Metal contacts were obtained by vacuum evaporation using a Leybold Heraus 300 Univex. The activation energy was measured using a Netes 6303D model power supply and a Nabertherm model oven.

3. Results and discussion

3.1. Structural properties

The XRD pattern of the ZnS film is shown in Fig. 1. The spectra were obtained by scanning 2θ in the range of 20°-70° with a grazing angle. In fig. 1, the diffraction peak originated at 2θ=29.5° (d=0.302 nm) corresponding to the (008) reflections of the hexagonal phase of ZnS. As determined from the position of the peak (008), lattice parameter c is estimated to be 2.42 nm. The calculated lattice parameter c is in agreement with the value from litrature; c=2.49 nm (JCPDF card no:39-1363). X-ray diffraction results agree well with those reported for ZnS [9,10] obtained on glass substrates by CBD at 80 °C. Some peaks observed in the ranges 20°-30° and 35°-40 are of much lower intensity than the (008) peak. The x-ray diffraction analysis showed that films are polycrystalline in nature.

The thicknesses of the films were calculated from the interference patterns around 400-800 nm as in our previous article [10]. The calculated thicknesses varied from 454 nm to 750 nm, and were obtained from maximum and minimum of the transmission curves.

The grain size of the ZnS films was found to be 35 nm for preferential orientations using the Debye-Scherer formula.

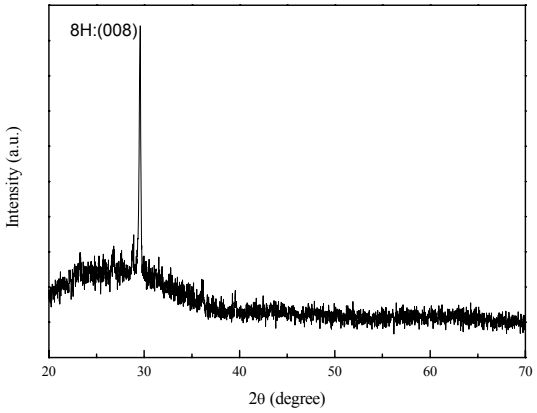

Fig. 1. The XRD pattern of the ZnS film deposited at 80 ºC.

3.2. Optical properties

The transmittance *(T)* and reflectance *(R)* spectrums of the ZnS thin films are shown in Fig. 2. The optical properties of ZnS thin films are determined from transmission measurements in the range 300-800 nm. Fig. 2a shows the transmission spectra of hexagonal ZnS thin films deposited at 80 °C with film thickness varying from 454 nm to 750 nm. The ZnS films showed high optical transmission (73-94 %) in the visible range.

The band gap values were calculated to be in the range of 3.79-3.93 eV in previous work [10]. These band gap values are higher than the bulk value of hexagonal ZnS because of quantum confinement in ZnS nanocrystals. This is consistent with literature [11].

The transmittance data was analyzed to determine the absorption coefficient, refractive index, extinction coefficient and dielectric constants. The refractive index n is a very important physical parameter related to the microscopic atomic interactions. From the theoretical point of view, there are basically two different approaches to this subject: on the one hand, considering the crystal as a collection of electric charges, the refractive index may be related to the density and the local polarizabilty of these entities [12]. On the other hand, considering the crystalline structure represented by a delocalized picture, the refractive index may be closely related to the energy band structure [13-15] of the material.

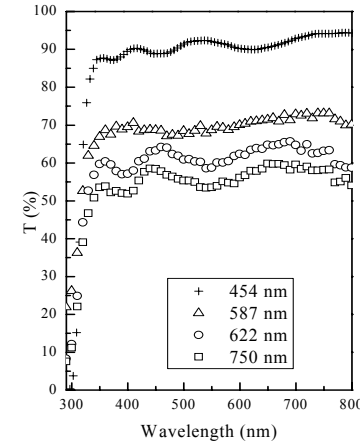

a

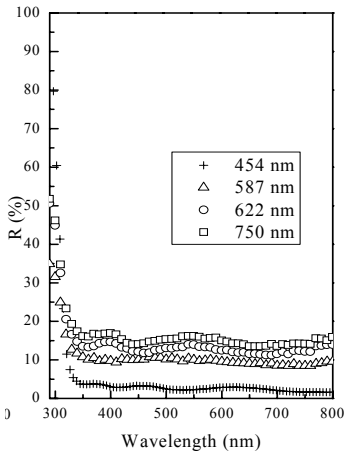

b

Fig. 2. The transmittance (a) and reflectance (b) spectra of the ZnS films of varying thicknesses obtained at 80 ºC.

Some optical values of the ZnS films such as reflection (*R*), absoption coefficient (*α*), extinction coefficient (*k*) and refractive index (*n*) were calculated from absorbance (*A*) and transmittance (*T*) spectra of the films by using the equations given below [16,17]:

$$T = 10^{-A},$$

$$\mathrm{I} = (1-\mathrm{R})^2(\mathrm{I_o e^{-\alpha d}}),$$

$$\alpha = \frac{\mathrm{A}}{\mathrm{d}}, \qquad \text{and} \qquad k = \frac{\alpha\lambda}{4\pi},$$

$$n = \frac{1+R}{1-R} + \sqrt{\frac{4R}{(1-R)^2} - k^2},$$

where *A* is the absorbance, *d* is the thickness of the film, I_o and *I* are the intensities of the incident and transmitted light respectively. The complex refractive index is expressed as:

$$n^*(\lambda) = n(\lambda) + ik(\lambda),$$

where *n* is the refractive index and *k* is the extinction coefficient. The dependence of the real part of the refractive index on the wavelength is shown in Fig. 3a. It can be seen that the real part of the refractive index decreases with increasing wavelength. The increase in the film thickness results increase in the refractive index. The refractive index *n* of the films with different thicknesses decreases from 2.05 to 1.35 at 550 nm wavelength. It is shown that the refractive index value of the ZnS film having thickness of 750 nm is 2.05. This value is closer to the corresponding bulk material (n=2.35) than the other refractive index values. The reason why refractive index values decrease from 2.05 to 1.35 might be attributed to the formation of non-stoichiometric oxide phases in the ZnS films [18].

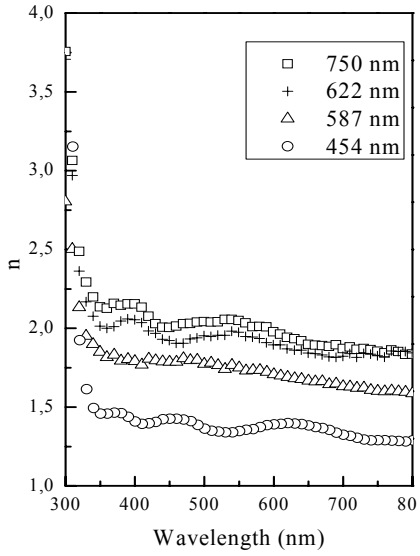

a

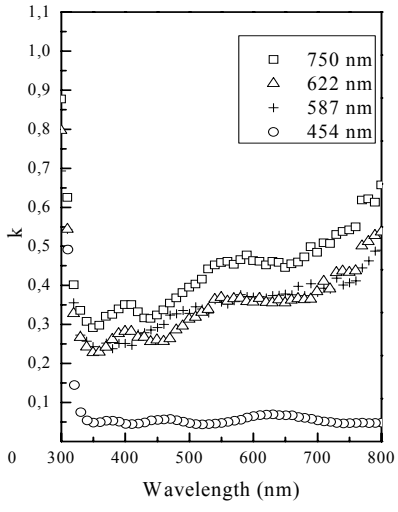

b

Fig. 3. The variation of refractive index (a) and extinction coefficient (b) with wavelength for ZnS films of different thicknesses obtained at 80 ºC.

In our previous results [10], the presence of higher atomic percentage of oxygen is revealed from the Energy dispersion x-ray (EDX) of the films. In [10], the atomic percentage of oxygen is increased slightly from 62.65 to 63.47. The average atomic ratios of S/Zn were calculated from the quantification of the peaks, giving values of 0.51, 0.56, 0.57 and 0.58 for different deposition times 3.0, 3.5, 4.0 and 4.5 h respectively. Our results are consistent with the literature [19] in which the ZnS films were deposited on a mono-crystalline silicon substrate with the concentration of thiourea at 80 ºC by CBD. The ZnS films formed by thiourea concentrations of 0.14 and 0.16 M have a refractive index of 2.05. After the annealing, the refractive index values of all the films reduced to the range 1.50-1.45.

The dependence of the imaginary part of the refractive index (*k*) on the wavelength is shown in Fig. 3b. It is observed that the extinction coefficient falls sharply till λ=317 nm and slowly increases above this wavelength. At 550 nm the extinction coefficient varies from 0.46 for the thickest film to 0.04 for the most thin film. Extinction coefficient values were found in the range 0.01-0.15 below the band gap edge [20] in which the cubic ZnS films were deposited by close-spaced evaporation (CSE) technique. Moreover, extinction coefficient values were changed from 0 to 0.60 below the band gap edge [21] in which the ZnS films were obtained by thermally evaporation.

It is well known that polarizability of any solid is proportional to its dielectric constant. The real and imaginary part of the complex dielectric constants are expressed below [22]:

$$\varepsilon_1 = n^2 - k^2,$$

$$\varepsilon_2 = 2nk,$$

where ε_1 is the real part and ε_2 is the imaginary part of the dielectric constant. The imaginary part confirms the contribution of the free carriers to the absorption. The real and imaginary part of the dielectric constants were calculated by using values of n and k with dielectric properties of the films changing with refractive index. The imaginary and real parts of the dielectric constant are directly related to the density of states within the forbidden gap of the compounds.

The dependence of the real part of the dielectric constant on the wavelength is shown in Fig. 4a. It shows that the real part of the dielectric constant decreases sharply between 300 and 317 nm and decreases slightly above 317 nm. The dependence of the imaginary part of the dielectric constant on the wavelength is shown in Fig. 4b generally increases slowly with wavelength for the range 350-800 nm.

The value of the optical dielectric constant ε_∞ was measured to be 5.7 in [23] for the hegzagonal ZnS. However, we calculated the maximum value of ε_∞ to be 4.2 using the formula $\varepsilon_\infty = n^2$ [24]. In ref. [25], the experimental value of ε_∞ was given as 5.1 for the cubic ZnS. ε_∞ values are higher than ours. The reason of this might be ascribed to the non-stoichiometric phase.

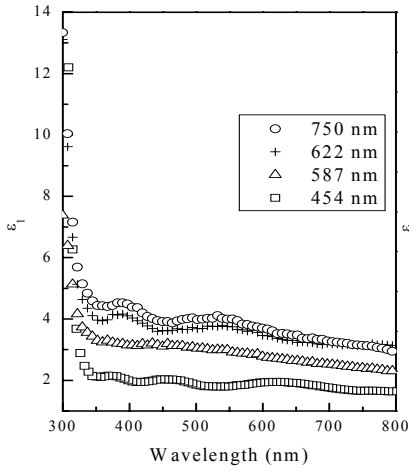

a

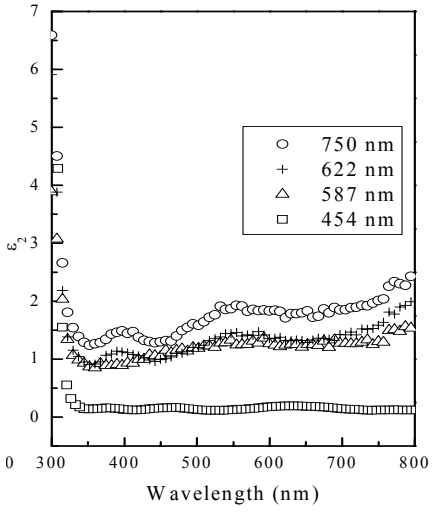

b

Fig. 4. The variation of the real (a) and imaginary (b) part of the dielectric constant with wavelength.

3.3. Electrical properties

I-V characteristics of the ZnS films before and after 1 hour of annealing at 400 ºC are shown in Fig 5. Surface type (planar) Au contacts were made for electrical measurements. The current values of the films were measured at room temperature and in the dark by applying voltage values between 0.1 and 100 V. The *I-V* variations of all the films are linear and neither space charge limited (SCL) nor trap filled limited (TFL) regions has been observed. Thus, the ohmic current mechanism is dominant for ZnS films. In the ohmic region, the number of free carriers is higher than the number of carriers injected into the semiconductor. So, the free carriers have a greater

effect on the current than injected carriers. When the *I-V* characteristic of ZnS films were investigated, it was seen that the current relationship to voltage was in the form of $I \sim V^{1.00}$ and ohmic conduction were dominant for the voltage range 0.1 - 100 V for the as-deposited film. For the annealed film, the relationship between current and voltage was in the form of $I \sim V^{0.92}$ and still ohmic conduction are dominant between 1 and 100 V.

The electrical conductivities of the films were calculated using Ohm's law given by:

$$J = \sigma E ,$$

where *J* is the electric current density, *(σ)* is the electrical conductivity and *E* is the electric field. The calculated electrical conductivity value is $1.62 \times 10^{-9} (\Omega.cm)^{-1}$ for the as-deposited film. This value is consistent with ref [26]. For the annealed film, electrical conductivity was calculated to be 1.32×10^{-10} $(\Omega.cm)^{-1}$. After annealing at 400 ºC the electrical conductivity of ZnS films decreased by about one order of magnitude. This low electrical conductivity or high resistivity is attributed to lattice defects and dislocations of the films and the results are in good agreement with the literature [27,28].

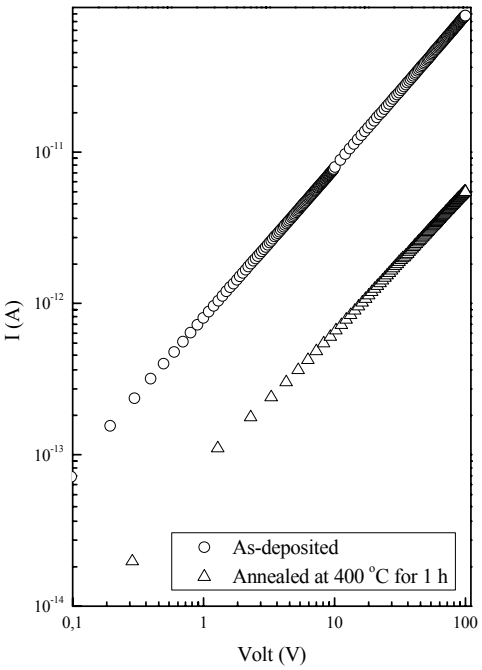

Fig. 5. The I-V characteristics of the ZnS films.

The activation energies of the film were evaluated using the following equation:

$$I = I_0 \exp\left(\frac{-E_a}{kT}\right),$$

where *I* is the current, E_a is the activation energy *k* is the Boltzman constant and *T* is the annealing temperature. In order to calculate the activation energies, ZnS films were heated in the oven by raising the temperature from 300 °K to 673 °K. The graphical representetion of $ln(I/I_0)$ versus 1000/T is given in Fig. 6. The plot of the logarithm of the current flow against *1000/T* yields a straight line with a slope of $-E_a/k$. The activation energies were calculated by this procedure.

The temperature dependence of current shows three different regions, ie., I, II and III, these regions arise from different conduction processes. In the low temperature region, region I (30-143 ºC), E_1 the activation energy value calculated to be 0.03 eV. In the high temperature region, region II (143-273 ºC) and region III (273-400 ºC), E_2 and E_3 were found to be 0.20 and 0.66 eV respectively.

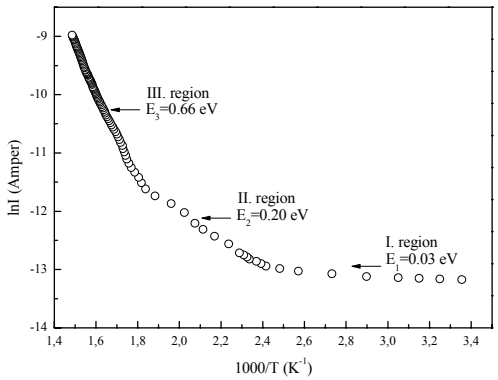

Fig. 6. The lnI versus 1000/T graphs of ZnS film deposited at 80 ºC.

In the present investigation, because the films were prepared by chemical bath deposition, oxygen molecules could be physically adsorbed onto the surface of the thin films as suggested from the EDX results in our previous work [10]. They then become chemisorbed having captured a conduction electron which binds them to the surface. The oxygen impurity can alter the microstructure of a growing film. The energy level of such a bound electron is sufficiently below the conduction band, that the electrons can easily escape from the trap levels to the conduction band with a very small amount of energy [29]. This could account for the low activation energies, which may be the energy required for a transition between the trap levels and the conduction band of the films. Consequently, the activation energy value of 0.03 eV could be attributed to shallow trap levels while activation energies which are 0.20 eV and 0.66 eV might be ascribed to deep and deeper trap levels respectively. The nature of the impurities responsible for the different values of activation energy requires further study.

4. Conclusions

The optical constants (refractive index *n*, extinction coefficient *k*, the real ε_1 and imaginary ε_2 parts of the dielectric constant) of ZnS films with varying thicknesses obtained by CBD at 80 ºC on glass substrates were analyzed from their transmittance and reflectance spectra.

The spectral dependence of the optical constant indicate that refractive index decreases with wavelength while extinction coefficient increases. It is shown that the maximal and minimal values of the refractive index at λ=550 nm were about 2.05 and 1.35. The electrical conductivity of the ZnS films decreased from $1.62x10^{-9}$ to $1.32x10^{-10}$ $(\Omega.cm)^{-1}$ when the films were annealed at 400 ºC for 1 hour. The evaluated activation energie values were 0.03 eV in the low temperature zone and 0.20 and 0.66 eV in the high temperature zones.

Acknowledgements

The authors would like to thank B. Royall for his contributions.

References

[1] R. O. Borges, D. Lincot, J. Videl, Proc. 11th Eur. Photovoltaic Sol. Energy Conf., Montreux, p. 862 (1992).
[2] H. Neumann, W. Horig, E. Reccius, H. Sobotta, B. Schumann, G. Kuhn, Thin Solid Films **61**, 13 (1979).
[3] H. C. Casey Jr., M.B. Panish, Heterostructure Lasers, Parts A and B, Academic Press, New York (1978).
[4] M. Rabah, B. Abbar, Y. Al-Douri, B. Bouhafs, B. Sahraoui, Mater. Sci. Eng. B **100**, 163 (2003).
[5] S. Lindroos, Y. Charreire, D. Bonnin, M. Leskela, Mater. Res. Bull. **33**, 453 (1998).
[6] E. J. Ibanga, C. Le Luyer, J. Mugnier, Mat. Chem. and Phys. **80**, 490 (2003).
[7] S. Wang, X. Fu, G. Xia, J. Wang, J. Shao, Z. Fan, Appl. Surf. Sci. **252**, 8734 (2006).
[8] G. Laukaitis, S. Lindroos, S. Tamulevičius, M. Leskelä, M. Račkaitis, Mater. Sci. and Eng. **A288**, 223 (2000).
[9] J. Cheng, D.B. Fan, H. Wang, B.W. Liu, Y.C. Zhang, H. Yan, Semicond. Sci. Technol. **18**, 676 (2003).
[10] F. Göde, C. Gümüş, M. Zor, J. Cryst. Growth **299**, 136 (2007).
[11] P. K. Ghosh, M. K. Mitra, K. K. Chatttopadhyay, Nanotechnol. **16,** 107 (2005).
[12] N. M. Balzaretti, J. A. H. da Jornada, Solid State Commun **99**, 943 (1996).
[13] James L. P. Hughes, J. E. Sipe, Phys. Rev. B **58**, 7761 (1998).
[14] A. Boukortt, B. Abbar, H. Abid, M. Sehil, Z. Bensaad, B. Soudini Mater. Chem. Phys. **82**, 911 (2003).
[15] T. Tsuchiya, S. Ozaki, S.Adachi, J. Phs: Condens. Matter. **15**, 3717 (2003).
[16] H. Kim, A. Pique, J. S. Horwitz, H. Murata, Z. H. Kafafi, C. M. Gilmore, D. B. Chrisey, Thin Solid Films **377-378**, 798 (2000).
[17] S. H. Brewer, S. Franzen, J. Alloys Compounds **338**, 73 (2002).
[18] O. L. Arena, M. T. S. Nair, P. K. Nair Semicond. Sci. Technol. **12**, 1323 (1997).
[19] U. Gangopadhyay, Kyunghae Kim, D. Mangalaraj, Junsin Yi, Appl. Surf. Sci **230**, 364 (2004).
[20] Y. P. Venkata Subbaiah, P. Prathap, K. T. Ramakrishna Reddy, Appl. Surf. Sci. **253**, 2409 (2006).
[21] S. M. A. Durrani, A. M. Al-Shukri, A. Iob, E. E. Khawaja, Thin Solid Films **379**, 199 (2000).
[22] T. Wiktorezyk, Thin Solid Films **405**, 238 (2002).
[23] Landolt-Bornstein, New Series III, Springer, Berlin, 1987.
[24] G. A. Samara, Phys. Rev. **B 27**, 3494 (1983).
[25] S. Q. Wang, J. Cryst. Grow. **287**, 185 (2006).
[26] C. Elbaum, Phys. Rev. Lett. **32(7),** 376 (1974).
[27] R. K. Nkum, A. A. Adimado, H. Totoe, Mater. Sci. Eng. B **55,** 102 (1998).
[28] R. Jeyakumar, S. T. Lakshmikumar, A. C. Rastogi, Vacuum **55** 71 (1999).
[29] J. C. Bailar, Jr., H. J. Emeléus, R. Nyholm, A. F. Trotman-Dickenson, Comprehensive Inorganic Chemistry, Pergamon, Oxford, vol. 2, p. 268,560-564, 710 (1973).

*Corresponding author: cgumus@cu.edu.tr